

See discussions, stats, and author profiles for this publication at: <https://www.researchgate.net/publication/47632456>

p67/MetAP2 Suppresses K-RasV12-Mediated Transformation of NIH3T3 Mouse Fibroblasts in Culture and in Athymic Mice

ARTICLE *in* BIOCHEMISTRY · OCTOBER 2010

Impact Factor: 3.02 · DOI: 10.1021/bi101225d · Source: PubMed

READS

51

5 AUTHORS, INCLUDING:



Avijit Majumdar

The Houston Methodist Research Institute

21 PUBLICATIONS 211 CITATIONS

SEE PROFILE

p67/MetAP2 Suppresses K-RasV12-Mediated Transformation of NIH3T3 Mouse Fibroblasts in Culture and in Athymic Mice[†]

Avijit Majumdar,^{‡,||} Arnab Ghosh,^{§,⊥} Samit Datta,^{§,@} Bethany C. Prudner,[‡] and Bansidhar Datta*,^{‡,§}

[‡]School of Biomedical Sciences and [§]Department of Chemistry and Biochemistry, Kent State University, Kent, Ohio 44242, United States. ^{||}Current address: Department of Pharmacology, Case Western Reserve University, Cleveland, OH 44106. [⊥]Current address: Department of Pathology, Cleveland Clinic Foundation, Cleveland, OH 44195. [@]Current address: M.D. Program, Tufts University School of Medicine, Boston, MA 02110.

Received August 2, 2010; Revised Manuscript Received October 28, 2010

ABSTRACT: In many tumor cells, the activation and activity of extracellular signal-regulated kinases (ERK1/2) are very high because of the constitutive activation of the Ras-mediated signaling pathway. Here, we ectopically expressed the human homologue of rat eukaryotic initiation factor 2-associated glycoprotein, p67/MetAP2, in EGF-treated mouse embryonic NIH3T3 fibroblasts and C2C12 myoblasts and NIH3T3 cell lines expressing the constitutively active form of MAP kinase kinase (MEK) to inhibit the activation and activity of ERK1/2 MAP kinases. In addition, we also ectopically expressed rat p67/MetAP2 in oncogenic Ras-induced transformed NIH3T3 fibroblasts and inhibited their transformed phenotype both in culture and in athymic nude mice possibly by inhibiting angiogenesis. This inhibition of ERK1/2 MAP kinases is due to the direct binding with rat p67/MetAP2, and this leads to the inhibition of activity of ERK1/2 MAP kinases both in vitro and in vivo. Furthermore, expression of p67/MetAP2 siRNA in both NIH3T3 fibroblasts and C2C12 myoblasts causes activation and activity of ERK1/2 MAP kinases. Our results thus suggest that ectopic expression of rat p67/MetAP2 in transformed cells can inhibit the tumorigenic phenotype by inhibiting the activation and activity of ERK1/2 MAP kinases and, thus, that p67/MetAP2 has tumor suppression activity.

Angiogenesis is the process of formation of blood vessels in which they either sprout or split from an existing blood vessel (1). Several small molecule inhibitors, including proteins and synthetic organic compounds with different chemical structures, have been shown to inhibit angiogenesis and cell growth (1, 2). Mammalian cell growth and proliferation are well-balanced because of the coordinated cellular events at the levels of DNA replication, transcription, and translation. Many of these cellular events are coupled to provide efficient control during normal cell growth and proliferation. Any deregulation of these well-balanced cellular processes pushes cells either into being removed from the organism via apoptosis or into abnormal growth toward tumorigenesis.

An anti-angiogenic drug, fumagillin, inhibits growth of endothelial cells (3), myoblasts (4), and several other cells (5). It covalently binds to the cellular target, methionine aminopeptidase 2 (MetAP2)¹ (6, 7), which shares ~95% sequence identity with a

eukaryotic initiation factor 2 (eIF2)-associated glycoprotein p67 (2). Thus, the new name of this protein is p67/MetAP2 (2). Because of the presence of intrinsic proteolytic activity, p67/MetAP2 undergoes autoproteolysis and generates several peptide fragments, among which the N-terminal p26 containing amino acid residues 1–107 is very stable (8). Another stable fragment containing downstream amino acid residues 108–480 has the catalytic pocket and the catalytic H231 site (7). The later site covalently binds to the anti-angiogenic drug, fumagillin (6, 7), and decreases the level of p67/MetAP2 autoproteolysis and increases its cellular level (4). The increased levels of p67/MetAP2 show a higher affinity for extracellular signal-regulated kinases 1 and 2 (ERK1/2) than eIF2α (4) and inhibit cell growth by inhibiting the cell signaling mediated by Ras (9). p67/MetAP2 binds directly with extracellular signal-regulated ERK1/2 MAP kinases in vivo and in vitro and inhibits their activation and activity (4, 10, 11). It also binds directly to α- and γ-subunits of eukaryotic initiation factor 2 (eIF2) and blocks the eIF2α-specific kinase(s), which phosphorylates eIF2α and reduces the rates of global protein synthesis (12, 13). Although it seems antagonistic, p67/MetAP2 coordinates well with the ERK1/2 MAP kinase cell signaling pathway and the protein synthesis machinery to provide effective yet novel communications between these two cellular processes to coordinate cell cycle and protein synthesis initiation (2).

The ERK1/2 MAP kinase pathway, when stimulated by epidermal growth factor (EGF) or platelet-derived growth factor (PDGF), regulates cell growth and proliferation, differentiation, and apoptosis (9). Deregulation of this pathway through constitutive activation due to specific mutations at (i) the receptor tyrosine kinase, EGFR (14), (ii) the proto-oncogene Ras (15),

[†]This work is supported in part by the Kent State University Research Council and a GSS research grant.

*To whom correspondence should be addressed: 014 SRL, Department of Chemistry and Biochemistry, Kent State University, Kent, OH 44242. Phone: (330) 672-3304. Fax: (330) 672-3816. E-mail: bdatta@kent.edu.

¹Abbreviations: ERK1/2, extracellular signal-regulated kinases 1 and 2; p-ERK1/2, phosphorylated forms of ERK1/2; EGF, epidermal growth factor; EGFP, enhanced green fluorescence protein; GFP, green fluorescence protein; MEKA, constitutively active form of MEK; RSK, ribosomal S6 kinase; MAP, mitogen-activated protein; p67, eIF2-associated glycoprotein; MetAP2, methionine aminopeptidase 2; GST, glutathione *S*-transferase; GST-MEK1, GST fusion of human MEK1; MBP, myelin basic protein; p-MBP, phosphorylated form of MBP; IP, immunoprecipitation; IB, immunoblotting; Ab, antibody.

(iii) Raf, a downstream effector of Ras (16), and (iv) MEK1/2, the downstream effectors of Raf (17), leads to tumorigenesis (9, 14–18). Because p67/MetAP2 binds directly to ERK1/2 MAP kinases and inhibits their activation and activity in vitro and in vivo, we asked whether overexpressing this protein in K-RasV12-transformed NIH3T3 fibroblasts will suppress tumorigenic phenotype in ex-vivo cell culture and in athymic nude mice. Our studies show that indeed ectopic expression of rat p67/MetAP2 inhibits the activation and activity of ERK1/2 MAP kinases induced by either EGF treatment or constitutively active MEK in both NIH3T3 fibroblasts and C2C12 myoblasts. It also suppresses K-RasV12-mediated transformed phenotypes of NIH3T3 fibroblasts both in culture and in athymic nude mice by inhibiting the activation and activity of ERK1/2 MAP kinases. The suppression of tumor growth in athymic nude mice due to overexpression of rat p67/MetAP2 possibly occurs via the inhibition of angiogenesis. Amino acid residues 76–358 of ERK1/2 MAP kinases bind directly to rat p67/MetAP2 at downstream amino acid residues 211–430 both in vitro and in vivo. These interactions inhibit rat p67/MetAP's autoproteolysis and ERK1/2 MAP kinase-mediated in vitro phosphorylation of myelin basic protein (MBP). In addition, expression of p67/MetAP2 siRNA causes induced activation and activity of ERK1/2 MAP kinases in both NIH3T3 fibroblasts and C2C12 myoblasts. Collectively, our data suggest that rat p67/MetAP2 has tumor suppression activity.

MATERIALS AND METHODS

Chemicals and Reagents. The chemicals used in this study were obtained from Sigma Chemicals (St. Louis, MO), Merck (Darmstadt, Germany), ICN Biomedicals, Inc. (Aurora, OH), Fisher Chemicals (Fairlawn, NJ), VWR (Chester, PA), and GIBCO-BRL (Rockville, MD). All enzymes used in this study were purchased from New England Biolabs (Beverly, MA). [γ -³²P]ATP was purchased from Amersham Corp. SuperFect transfection reagent and Ni²⁺-NTA agarose beads were from Qiagen. Glutathione agarose beads were purchased from Sigma Chemicals, and glutathione agarose bead-bound GST-ERK1, GST-MEK1, and myelin basic protein were purchased from Upstate Biotechnology (Lake Placid, NY). Kinase active ERK1 and ERK2 were purchased from Bioline and New England Biolabs (Beverly, MA), respectively. Cell culture media and fetal bovine serum were purchased from GIBCO/Invitrogen Life Science Biotechnology. Fetal calf serum used for culturing NIH3T3 fibroblasts was obtained from Colorado Serum Co. (Boulder, CO).

Plasmid Construction. The plasmids encoding Flag epitope-tagged ERK1 and ERK2 were gifts from S. Eblen and A. Catling (University of Texas at San Antonio, San Antonio, TX). The hemagglutinin (HA)-tagged MEKA construct was a kind gift from N. Ahn [University of Colorado, Boulder, CO (17)], and the oncogenic K-RasV12 was a kind gift from A. Wolfman (Cleveland Clinic Foundation, Cleveland, OH). The pZip empty vector was obtained from the pZip-K-RasV12 plasmid after restriction digestion with BamHI to take out the K-RasV12 insert followed by self-ligation. The construction of plasmids expressing enhanced green fluorescence protein (EGFP) tagged with rat p67/MetAP2 and Myc epitope-tagged rat p67/MetAP2 has been described previously (4, 10, 11, 19, 20). Full-length p67/MetAP2 and its various deletion mutants were subcloned into the pCMV-Myc vector in the Bg/II and NotI sites. His-tagged p67/MetAP2

and its deletion mutants, p52 (encoding amino acid residues 108–480) and p26 (encoding amino acid residues 1–107), were purified from baculovirus-infected Sf21 insect cells following the procedures described previously (4, 8). The GST fragments of p67/MetAP2 were obtained by subcloning the respective cDNA encoding the fragments into the BamHI and EcoRI sites of GST expression vector pGEX-1X. The GST fragments of ERK1 and ERK2 were obtained by subcloning the respective cDNA encoding the fragments into BamHI and EcoRI sites for ERK1 and BamHI and NotI sites for ERK2, respectively, of GST expression vector pGEX-4T1.

Antibodies. Mouse monoclonal antibodies specific for p-ERK1/2 (Sc-7383), ERK2 (Sc-1647), MEK1 (Sc-6250), p-MEK1/2 (Sc-7995), K-Ras (Sc-30), p-RSK (Sc-12898), and cyclin D1 (Sc-20044) were obtained from Santa Cruz Biotechnology (Santa Cruz, CA). The anti-FLAG M2 monoclonal antibody specific for the Flag epitope and the monoclonal antibody specific for α -actin were purchased from Sigma Chemicals. The anti-Myc and anti-HA antibodies were obtained from Clontech (Mountain View, CA) in a kit containing the pCMV-Myc and pCMV-HA vectors. Rabbit polyclonal antibodies specific for ERK1 (Sc-94) were obtained from Santa Cruz Biotechnology. ERK1 polyclonal antibodies recognize both ERK1 and ERK2 on Western blots. Similarly, a monoclonal antibody specific for the phosphorylated forms of ERK1/2 recognizes the phosphorylated forms of both ERK1 and ERK2. A monoclonal antibody specific for EGFP was purchased from Clontech. Mouse monoclonal antibodies specific for His (Sc-8036) and GST (Sc-138), rabbit polyclonal antibodies specific for ERK1 (Sc-94), and the monoclonal antibody specific for pRb (Sc-65230) were obtained from Santa Cruz Biotechnology.

Cell Culture. C2C12 mouse myoblasts (ATCC, CRL-1172) were cultured in Dulbecco's modified Eagle's medium (DMEM) containing 100 units/mL penicillin/streptomycin (GIBCO/BRL) and 10% fetal bovine serum (GIBCO/Invitrogen). Cells were maintained at 37 °C in a humidified 8% CO₂ incubator. NIH3T3 cells (ATCC, CRL-1658) were maintained in DMEM supplemented with 10% fetal calf serum and antibiotics at 37 °C in the presence of 8% CO₂ and 92% air following the supplier's protocol.

Generation of the Stable NIH3T3 Cell Line. NIH3T3 cells (60–70% confluent) were transfected with expression vector, pZip, and plasmid expressing oncogenic K-RasV12 or EGFP alone or EGFP-tagged rat p67/MetAP2 using the Superfect transfection reagent following the manufacturer's protocol (Qiagen). Forty hours after transfection, cells were trypsinized, split into multiple culture dishes, and maintained in growth medium containing G418 for 14 days. After 14 days, the individual colonies (100–200) were pulled together and maintained in the presence of G418.

Transient Transfection. An NIH3T3 cell line (60–70% confluent) carrying the pZip expression vector or the transformed NIH3T3 cells were transfected with plasmids expressing Myc-tagged rat p67/MetAP2, HA-tagged MEKA, EGFP-tagged rat p67/MetAP2, and EGFP empty vector as indicated using the Superfect transfection reagent following the manufacturer's protocol (Qiagen). Cell lysates were made 40 h after transfection as described previously (4, 10, 11, 19, 20).

Measurement of Transfection Efficiency. The transfection efficiency was measured by using the β -galactosidase staining kit (Mirus Bio, LLC, Madison, WI) following the manufacturer's protocol. In brief, after transfection, cells were fixed on coverslips

via incubation with 50% glutaraldehyde, stained with staining solution containing X-Gal reagent, and incubated for 1 h at 37 °C in an area protected from light. The blue stained cells were then counted by using light microscopy. The transfection efficiency is determined by calculating the ratio of blue-stained cells to total cells. These transient transfection efficiencies vary from 40 to 50%. In some cases, efficiencies seemed to be higher. This procedure is routinely used for the measurement of the transfection efficiency of mammalian cells (21).

Analysis of the Growth Rate. NIH3T3 cells carrying the pZip expression vector, oncogenic K-RasV12-transformed NIH3T3 cells alone or transfected with an EGFP vector, or a plasmid expressing the EGFP-tagged rat p67/MetAP2 isoform were seeded at a density of 1×10^5 cells/60 mm culture dish in growth medium and incubated at 37 °C. The number of cells was counted in a hemocytometer every day up to 5 days from the day of seeding. These experiments were performed in triplicate for each time interval.

Analysis of the Serum Dependence. The serum dependence was determined by seeding NIH3T3 cells carrying the pZip expression vector, oncogenic K-RasV12-transformed NIH3T3 cells alone or transfected with EGFP vector, and a plasmid expressing EGFP-tagged rat p67/MetAP2 at a density of 1×10^5 cells/60 mm culture dish and allowing the cells to attach for 5 h in growth medium supplemented with 10% calf serum. The media on the dishes were then changed to growth medium supplemented with 1% calf serum. The numbers of cells were counted in a hemocytometer every 2 days, and the medium was changed every 2 days up to 6 days. These experiments were performed in triplicate for each time interval.

Focus Formation Assay. NIH3T3 cells carrying the pZip expression vector, oncogenic K-RasV12-transformed NIH3T3 cells alone or transfected with EGFP vector, and a plasmid expressing EGFP-tagged rat p67/MetAP2 were seeded at a density of 1×10^5 cells/60 mm culture dish in growth medium and incubated at 37 °C. The medium was changed every 3 days. After 10 days, cells were fixed in a phosphate-buffered saline (PBS) solution containing 0.2% glutaraldehyde and 0.5% formaldehyde for 10 min on ice and stained with 0.2% crystal violet for 10 min at room temperature. The number of foci was counted. These experiments were conducted in triplicate at three sets.

Studies in Athymic Mice. NIH3T3 cells carrying the pZip expression vector and oncogenic K-RasV12-transformed NIH3T3 cells were seeded at a density of 1×10^5 cells/100 mm culture dish containing growth medium and incubated at 37 °C in an incubator. When cells on plates reached ~50–60% confluence, they were transfected with EGFP vector and a plasmid expressing EGFP-tagged rat p67/MetAP2 using superfect transfection reagent (Qiagen). After being transfected for 40 h, cells were collected by trypsinization, and a cell suspension of 0.2 mL was made. For tumor formation in athymic nude mice, 10^6 cells were injected subcutaneously into both the flanks of mice using a 21-gauge needle. Thirteen days after injection, mice were sacrificed and the tumors were collected and weighed.

Hematoxylin and Eosin Staining. Tumor slices were made, fixed on coverslips, and stained with Hematoxylin and Eosin following the procedures described previously (21).

Cell Lysate Preparation, Immunoblotting, and Co-Immunoprecipitation Assays. Cell lysates were made after cells had been harvested; protein concentrations were measured, and cell lysates were subjected to SDS-PAGE and transferred to nitrocellulose filters. The immunoblotting experiments and

co-immunoprecipitation assays were performed using different antibodies as described previously (4, 8, 10, 11, 19, 20).

In Vitro Binding Assays. The binding of purified His-p67/MetAP2 and ERK1 and ERK2 was performed in the wash buffer following the procedures as described previously (4). In brief, for immobilization of His-p67/MetAP2 in Ni-NTA agarose beads, beads were washed, purified His-p67/MetAP2 was added, and the binding was conducted at 4 °C. The unbound His-p67/MetAP2 was removed by microcentrifugation, and GST-ERK1 or purified ERK2 was added to the beads. As a control, a purified GST sample was used to detect nonspecific interaction with His-p67/MetAP2. The mixtures were rotated at room temperature for 2 h, microcentrifuged, and washed extensively with ample amounts of wash buffer. To the beads were added 5× loading dye and the SDS running buffer, and the mixture was boiled for 10 min. After a brief microcentrifugation, the supernatants were loaded on a 15% SDS-PAGE gel. The proteins from the gel were transferred to a nitrocellulose membrane and detected by immunoblotting with appropriate antibodies. For the binding of the GST-tagged p67/MetAP2 fragments with ERK1 and ERK2, the same procedure was followed except the GST fragments of p67/MetAP2 were immobilized by being bound in the glutathione-agarose beads and kinase active ERK1 or ERK2 was added on top. For the binding of the GST-tagged ERK2 fragments with His-p67/MetAP2, the same procedure was followed as described except the GST fragments of ERK2 were immobilized by being bound in the glutathione agarose beads and His-p67/MetAP2 was added on top. Purified GST protein was used as a control. Similar GST pull-down assays were performed with purified GST-MEK1.

In Vitro Kinase Assay of Myelin Basic Protein (MBP) by the GST-ERK1 and purified ERK2. In a typical phosphorylation assay, 0.5 µg of MBP was phosphorylated by the bound activated GST-ERK1 or 6 ng of ERK2 in the presence of 50 mM Tris-HCl (pH 7.5), 10 mM MgCl₂, 1 mM EGTA, 2 mM DTT, 0.01% Brij 35, and 40 µM ATP. The reaction was initiated via addition of 10 µCi of [γ -³²P]ATP (specific activity of 3500 Ci/mmol, Amersham) and incubation at 30 °C for 30 min. The reactions were stopped via addition of 5× SDS loading dye and the mixtures boiled for 10 min. The denatured samples were analyzed via 15% SDS-PAGE followed by autoradiography or transferred to a nitrocellulose membrane for immunoblot analyses.

RESULTS

Rat p67/MetAP2 Suppresses K-RasV12-Mediated Transformation of NIH3T3 Mouse Fibroblasts in Cell Culture and in Athymic Mice by Inhibiting Activation and Activity of ERK1/2 MAP Kinases. Enhanced phosphorylation of ERK1/2 MAP kinases provides a growth-promoting signal to mammalian cells (22), and the master regulator for this signal cascade pathway is the proto-oncogene product, Ras (15, 23). Mutation of Ras at positions 12, 13, and 61 causes transformation of mammalian cells and ultimately leads to tumorigenesis (23, 24). p67/MetAP2 binds to ERK1/2 and inhibits their activation and activity in C2C12 mouse myoblasts (4, 10, 11). To test whether rat p67/MetAP2 can inhibit the transformation phenotype of NIH3T3 mouse fibroblasts, we transiently over-expressed p67/MetAP2 in NIH3T3 mouse fibroblasts constitutively expressing K-RasV12 and examined their phenotypes (Figure 1). K-RasV12-expressing NIH3T3 fibroblasts started colonizing before reaching confluence and formed large foci when

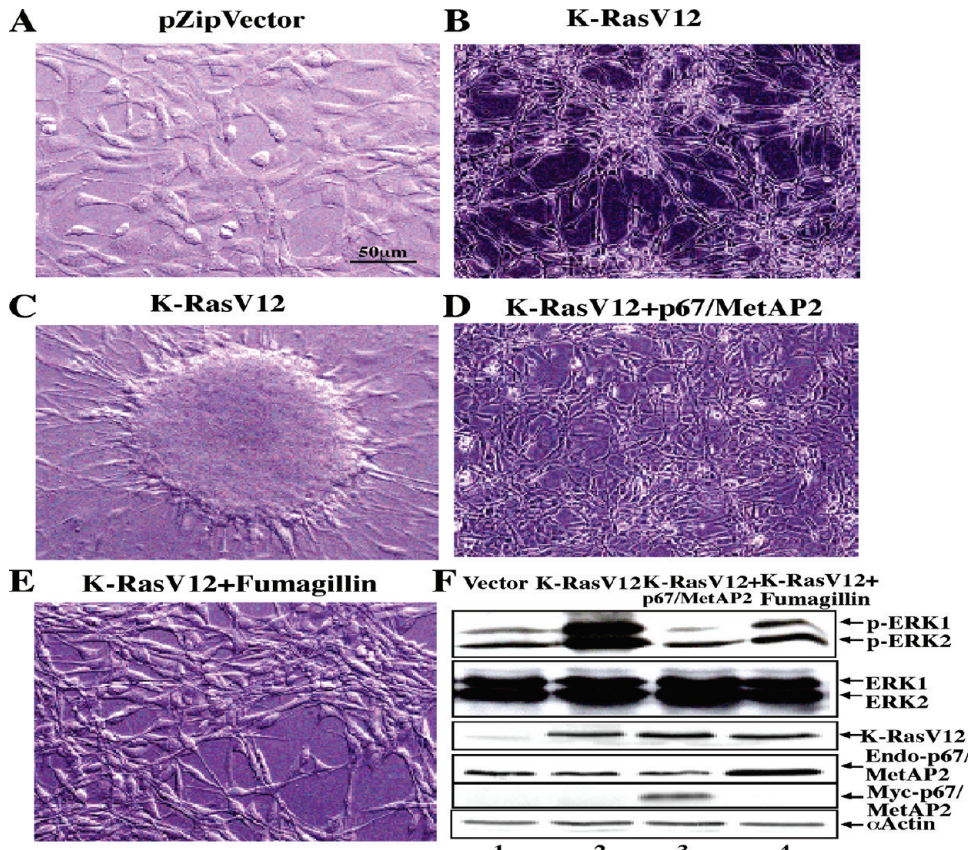


FIGURE 1: Rat p67/MetAP2 inhibits the transformation phenotype and activation of ERK1/2 MAP kinases in NIH3T3 fibroblasts constitutively expressing oncogenic K-RasV12. Stable NIH3T3 cell lines constitutively expressing the pZip vector (A) and pZip vector-containing oncogenic K-RasV12 (B) were generated. K-RasV12-transformed cells when kept in a culture dish for an additional 3 days formed foci (C) but showed a reduced number of foci when they were transiently transfected with a plasmid expressing Myc-tagged rat p67/MetAP2 (D). Transformed NIH3T3 fibroblasts as shown in panel B after being treated with 10 μ M fumagillin also showed a reduced number of foci (E). Cells were examined under the microscope at 50 μ m magnification. Lysates from all the cell lines shown above were analyzed for the levels of the phosphorylated forms of ERK1/2 (F, panel 1 from the top), total ERK1/2 (panel 2), K-RasV12 (panel 3), endogenous p67/MetAP2 (panel 4), Myc-p67/MetAP2 (panel 5), and, as a loading control, α -actin (panel 6) by Western blots.

grown for several days in Petri dishes as compared to control cells carrying the expression vector, pZip (compare Figure 1A–C). Transient overexpression of rat p67/MetAP2 in K-RasV12-transformed NIH3T3 fibroblasts significantly inhibited their colonization and formation of foci (Figure 1D). Because the treatment of endothelial cells, mouse myoblasts, and mouse fibroblasts with fumagillin, an anti-angiogenic drug, decreases turnover rates of p67/MetAP2 and increases its endogenous level, we treated K-RasV12-transformed NIH3T3 fibroblasts with fumagillin and examined the cells' phenotypes. The phenotype of K-RasV12-expressing cells treated with fumagillin changed toward normal that is very similar to the pZip vector-expressing cells (compare panels A, B, and E of Figure 1). Analyses of the phosphorylated forms of ERK1/2 showed an 8–10-fold increase in the level of K-RasV12-expressing cells, and this increased level of phosphorylation was reduced to a level below the control level when rat p67/MetAP2 was transiently overexpressed in these transformed cells (in Figure 1F, compare lanes 1–3). Fumagillin treatment also reduced the phosphorylation levels of ERK1/2 MAP kinases to a level near the control level (Figure 1F, lane 4), and this correlates with the increased levels of p67/MetAP2 in fumagillin-treated cells as compared to pZip vector-expressing control cells (in Figure 1F, compare lanes 1 and 4, second panel from the bottom). The expression of K-RasV12 was unchanged during the transient overexpression of p67/MetAP2 or treatment with fumagillin (Figure 1F, lanes 2–4, third panel from the top), and the total

ERK1/2 level was also the same in cell lines tested in these experiments (Figure 1F, second panel from the top). Collectively, our data suggest that increased levels of p67/MetAP2 significantly inhibited K-RasV12-mediated activation of ERK1/2 MAP kinases in NIH3T3 fibroblasts and suppressed the transformed phenotype of these cells.

To examine whether the suppression of the transformed phenotype mentioned above is also observed in athymic mice, we injected K-RasV12-transformed NIH3T3 cells at both the left and right sides of the dorsoventral lining in athymic mice. Two days prior to the injection, K-RasV12-expressing NIH3T3 cells were transiently transfected with either EGFP expression vector or plasmid expressing EGFP-tagged rat p67/MetAP2. Five days after injection, mice bearing K-RasV12-transformed cells developed tumors whereas the same transformed cells overexpressing rat p67/MetAP2 developed smaller size tumors 8 days after injection (Figure 2A–D). Well-grown tumors were excised (Figure 2E) from individual mice after injection for 13 days and weighed (Figure 2F). The average weight of the tumor generated from K-RasV12-transformed cells was 4.0 g, whereas this average was reduced to 0.9 g when rat p67/MetAP2 was overexpressed in the transformed cells before injection into nude athymic mice (Figure 2F). Our analyses of the tumor slices from xenograft mice by staining with Hematoxylin and Eosin (H&E) indicated that cells from K-RasV12 tumors exhibited much stronger Hematoxylin staining as compared to tumors obtained

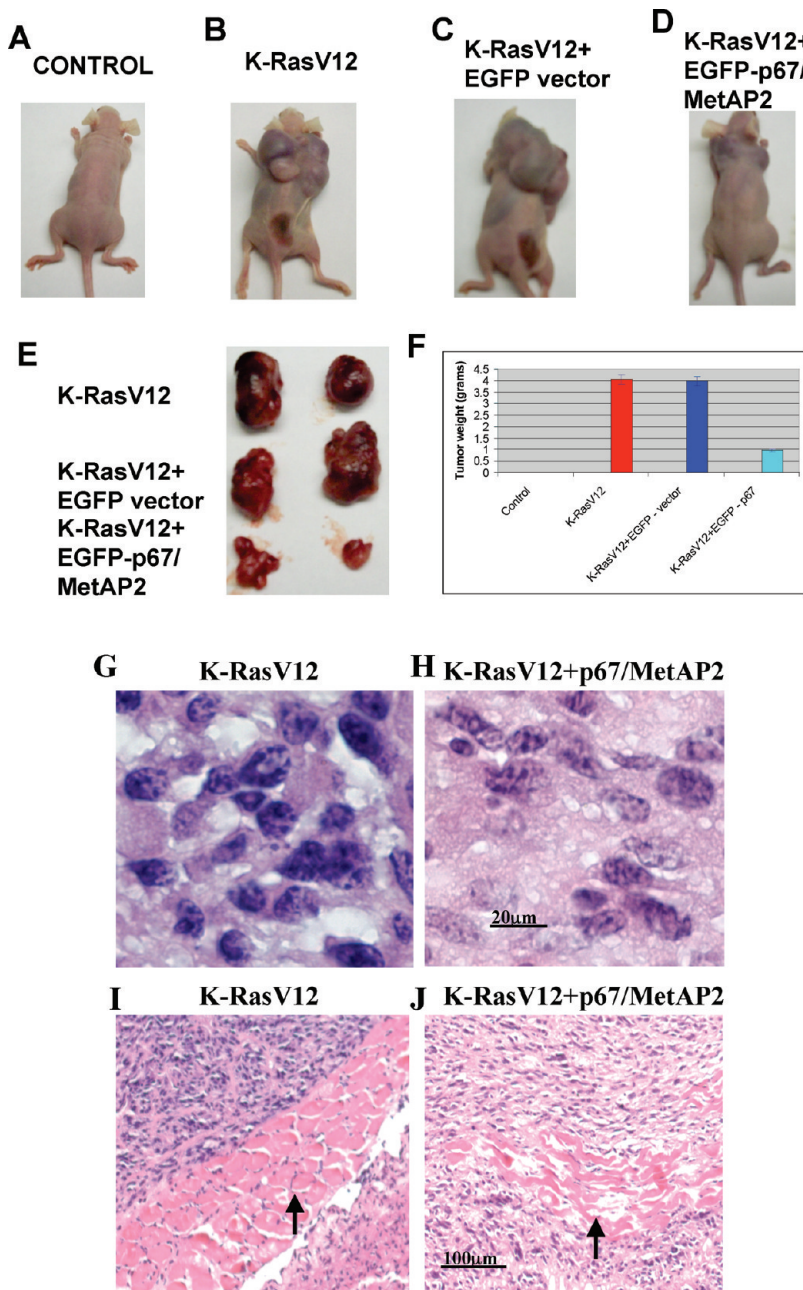


FIGURE 2: Ectopic expression of rat p67/MetAP2 regresses the growth of tumors formed by NIH3T3 fibroblasts constitutively expressing oncogenic K-RasV12 in athymic mice. NIH3T3 fibroblasts constitutively expressing oncogenic K-RasV12 were transiently transfected with EGFP vector or a plasmid expressing EGFP-tagged rat p67/MetAP2 2 days prior to injection. Cells were trypsinized and injected subcutaneously in both the dorsal flanks of the athymic nude mice on either side of the midline. After injection for 13 days, mice were sacrificed (A–D) and tumors were excised surgically (E) and weighed (F). Paired two-tail *t* tests were performed for the comparison between oncogenic K-RasV12-transformed cells expressing EGFP alone and oncogenic K-RasV12-transformed cells expressing EGFP-tagged rat p67/MetAP2 (asterisk), giving the *p* value of 0.00024. (A) Mice were treated with NIH3T3 fibroblasts carrying the pZip vector. (B) Mice were treated with NIH3T3 fibroblasts constitutively expressing K-RasV12. (C) Same as panel B but transiently transfected with the EGFP vector. (D) Same as panel B but ectopically expressing EGFP-tagged rat p67/MetAP2. For each injection, a total of three 4-week-old female athymic mice were used, and the whole procedures were repeated twice. (G–J) Xenograft tumors were surgically removed, and thin layer tumor slices were fixed on coverslips, stained with H&E dyes, and examined under a microscope. Cells in panels G and H were examined at 100 \times magnification, whereas cells in panels I and J were examined at 20 \times magnification. In panels I and J, red blood cells are stained red. A well-developed invasive blood vessel (vertical arrow) is seen diagonally in panel I, whereas a thin and poorly developed blood vessel (vertical arrow) is seen horizontally in panel J.

from K-RasV12-transformed cells overexpressing rat p67/MetAP2 (in Figure 2, compare panels G and H). In contrast, the Eosin staining showed very little difference between the two tumor slices described above. These results indicate that cells from K-RasV12 tumors are proliferating at a faster rate than cells in tumors suppressed by rat p67/MetAP2. The H&E staining also revealed well-grown blood vessels invaded the solid tumors

developed from K-RasV12-mediated transformed NIH3T3 fibroblasts (Figure 2I) and poorly matured blood vessels invaded the solid tumors that were developed from K-RasV12-mediated transformed NIH3T3 fibroblasts ectopically expressing rat p67/MetAP2 (Figure 2J). Altogether, these results suggest that ectopic expression of rat p67/MetAP2 in transformed NIH3T3 fibroblasts suppresses tumor development, possibly by inhibiting

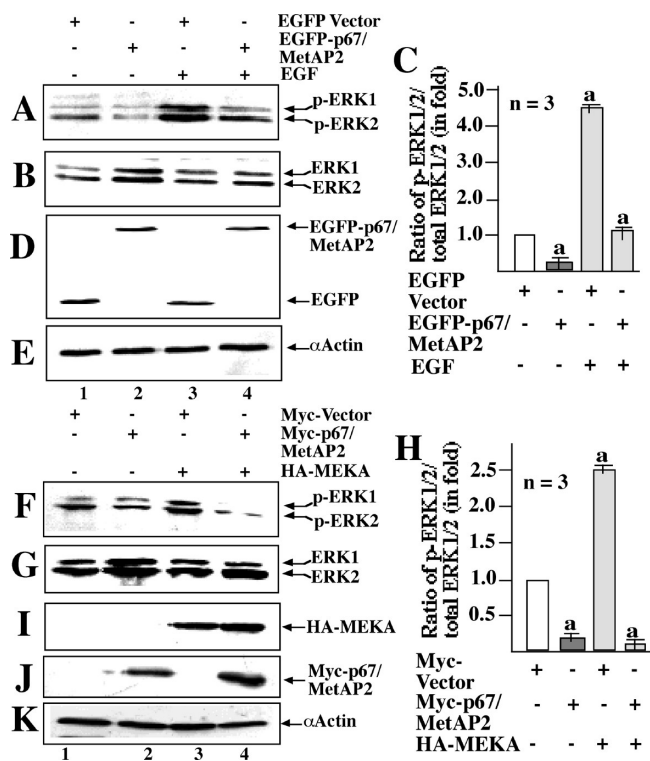


FIGURE 3: Rat p67/MetAP2 inhibits EGF-stimulated activation and constitutively active MEK-stimulated activation of ERK1/2 in NIH3T3 mouse fibroblasts. Overnight serum-starved NIH3T3 fibroblasts constitutively expressing EGFP or EGFP-tagged rat p67/MetAP2 were treated with epidermal growth factor (EGF) for 10 min. Cell lysates from treated and untreated cells were analyzed for the levels of the phosphorylated forms of ERK1/2 (A), total ERK1/2 (B), EGFP or EGFP-tagged p67/MetAP2 (D), and α -actin as a loading control (E) on Western blots. Bands from panels A and B were scanned to measure the ratios of the phosphorylated forms of ERK1/2 and total ERK1/2, and the relative fold increase was calculated using NIH Image quant-162 (C). The data were analyzed using a one-way ANOVA, and p values of <0.05 were considered significant. NIH3T3 fibroblasts expressing Myc vector (lane 1), Myc-p67/MetAP2 (lane 2), HA-MEKA (lane 3), or both Myc-p67/MetAP2 and HA-MEKA (lane 4) were analyzed for the levels of the phosphorylated forms of ERK1/2 (F), total ERK1/2 (G), HA-MEKA (I), Myc-p67/MetAP2 (J), and α -actin (K) as a loading control on immunoblots. The analyses (H) were performed in a manner similar to that described above, and p values of <0.01 were considered significant.

the formation of new blood vessels or angiogenesis. This inhibition of blood vessel formation is due to the inhibition of activation and activity of ERK1/2 MAP kinases by p67/MetAP2.

To confirm this, we examined the ratio of the phosphorylated forms and the total of ERK1/2 MAP kinases in two stable cell lines: one expressing expression vector EGFP and the other expressing EGFP-tagged rat p67/MetAP2 (Figure 3). There was a more than 5-fold decrease in the level of phosphorylation of ERK1/2 MAP kinases in cells expressing EGFP-tagged rat p67/MetAP2 than control vector-expressing cells (in Figure 3A–C, compare lanes 1 and 2). EGF treatment of expression vector-carrying cells showed a 4.5-fold increase in the level of ERK1/2 phosphorylation, and 70% of this increased level of phosphorylation was suppressed when rat p67/MetAP2-expressing NIH3T3 cells were treated with EGF (Figure 3A–C, lane 4). In stable cell lines, the level of EGFP-p67/MetAP2 was only 40–50% of its endogenous level (data not shown). Because levels of ectopically expressed rat p67/MetAP2 (Figure 3D) and α -actin

(Figure 3E), a loading control, remain basically unchanged in these two cell lines, these results suggest that EGF-induced activation of ERK1/2 MAP kinases is suppressed when rat p67/MetAP2 is constitutively expressed in NIH3T3 mouse fibroblasts. To provide another line of evidence that shows that indeed rat p67/MetAP2 is inhibiting the phosphorylation of ERK1/2 MAP kinases, we ectopically expressed a constitutively active form of MEK, called MEKA (17), in NIH3T3 fibroblasts to activate ERK1/2 MAP kinases, and for these cells rat p67/MetAP2 was transiently expressed. Consistent with our earlier observation, the basal level of phosphorylation of ERK1/2 was inhibited more than 80% by transient expression of Myc-tagged rat p67/MetAP2 (in Figure 3F–H, compare lanes 1 and 2). Transient expression of MEKA showed a 2.5-fold increased level of phosphorylation of ERK1 compared to that of ERK2 (Figure 3F, lane 3); however, the phosphorylation of both ERK1/2 was inhibited by more than 90% when Myc-tagged rat p67/MetAP2 was ectopically expressed in NIH3T3 mouse fibroblasts (compare lane 3 with lane 4 in Figure 3F–H). Because the expression of HA-tagged MEKA (Figure 3I, lanes 3 and 4), Myc-tagged p67/MetAP2 (Figure 3J, lanes 2 and 4), and a loading control α -actin (Figure 3K) basically remained unchanged, these results led us to conclude that rat p67/MetAP2 inhibits MEK-mediated activation of ERK1/2 MAP kinases.

We also examined the effects of overexpression of p67/MetAP2 on phosphorylation of MEK, which is the upstream activator, and RSK, which is the downstream effector of ERK1/2 MAP kinases, in K-RasV12-transformed NIH3T3 fibroblasts (Figure 4). Our analyses showed a 12-fold increase in the level of MEK phosphorylation in K-RasV12-transformed cells as compared to control NIH3T3 fibroblasts carrying the pZip expression vector alone (in Figure 4A–C, compare lanes 1 and 3). Overexpression of rat p67/MetAP2 in control cells reduced the level of MEK phosphorylation by 50% (in Figure 4A–C, compare lanes 1 and 2), whereas >95% inhibition was noticed in K-RasV12-transformed cells (in Figure 4A–C, compare lanes 3 and 4). Among several downstream targets of ERK1/2 MAP kinases, phosphorylation of RSK leads to the stimulation of protein synthesis (25–28), whereas the increased level of cyclin D1 is involved in cell cycle progression (29). Our examination of levels of phosphorylation of RSK as compared to its total amounts in K-RasV12-mediated transformed NIH3T3 fibroblasts showed 12-fold higher levels compared to those of control NIH3T3 fibroblasts carrying expression vehicles pZip and EGFP (in Figure 4D–F, compare lanes 1 and 3). These phosphorylation levels were, however, decreased to 10 and 8%, respectively, when rat p67/MetAP2 was transiently overexpressed in the control NIH3T3 fibroblasts carrying pZip expression vehicle (Figure 4D–F, lane 2) and K-RasV12-transformed cells (Figure 4D–F, lane 4). Examination of the levels of cyclin D1 in the two cell lines described above also revealed that the level was increased by 8-fold in K-RasV12-mediated transformed NIH3T3 fibroblasts as compared to control cells carrying expression vehicles pZip and EGFP (in Figure 4G,H, compare lanes 1 and 3), and this level was suppressed to less than 5 and 50%, respectively, when rat p67/MetAP2 was transiently overexpressed in these two cell lines (in Figure 4G,H, compare lane 1 with lane 2 and lane 3 with lane 4). Because the expression of K-RasV12 (Figure 4I, lanes 3 and 4), EGFP-tagged rat p67/MetAP2 (Figure 4J, lanes 2 and 4), and a loading control, α -actin (Figure 4K), remained unchanged, these data suggest that rat p67/MetAP2 can suppress the phosphorylation of MEK1 and

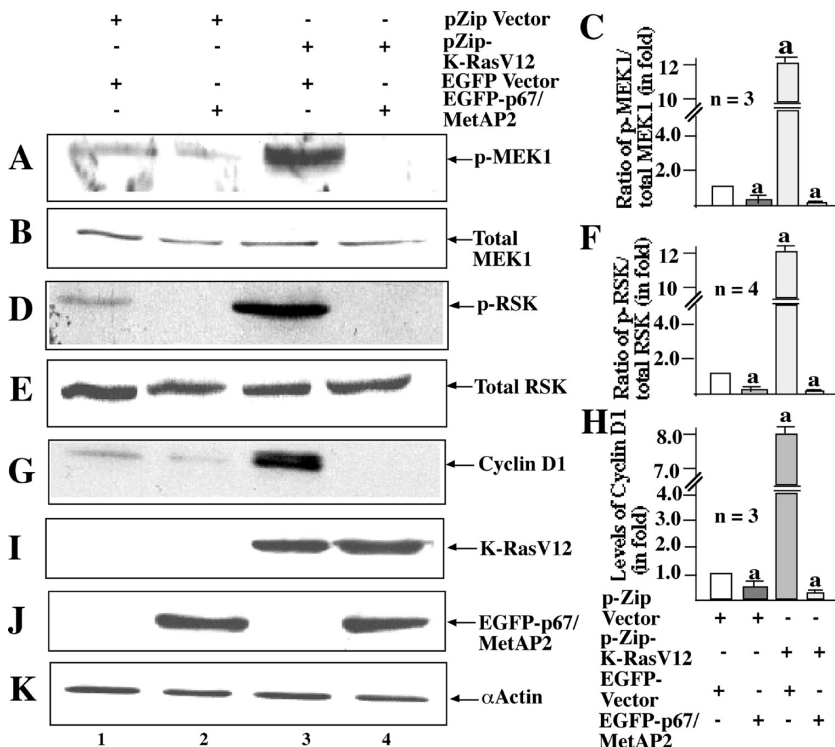


FIGURE 4: Rat p67/MetAP2 inhibits the phosphorylation of MEK and RSK and lowers the level of cyclin D1 in K-RasV12-mediated transformed NIH3T3 mouse fibroblasts. NIH3T3 cell lines constitutively expressing the pZip vector (lanes 1 and 2) or pZip vector containing oncogenic K-RasV12 (lanes 3 and 4) were transiently transfected with empty vector expressing EGFP (lanes 1 and 3) or a plasmid expressing EGFP-p67/MetAP2 (lanes 2 and 4). Cells were harvested, and lysates from these lines were analyzed for the levels of the phosphorylated form of MEK1 (A), total MEK1 (B), the phosphorylated form of RSK (D), and total RSK (E), and levels of cyclin D1 (G), K-RasV12 (I), EGFP-tagged rat p67/MetAP2 (J), and α -actin as a loading control (K) on Western blots. Bands corresponding to the phosphorylated form of MEK and its total (A and B, respectively), the phosphorylated form of RSK and its total (D and E, respectively), and levels of cyclin D1 (G) were scanned, and analyses were performed (C, F, and H, respectively) following procedures similar to those mentioned in the legend of Figure 3, *p* values of <0.035–0.05 were considered significant. The faster-migrating EGFP protein in lanes 1 and 3 is not shown.

RSK and levels of cyclin D1 significantly in K-RasV12-mediated NIH3T3 transformed mouse fibroblasts.

The important characteristics of transformed cells are their higher growth rates, their ability to grow in low-serum media, and their ability to form foci as compared to nontransformed cells (9). Indeed, the tumorigenic K-RasV12-transformed NIH3T3 fibroblasts showed increased growth rates (Figure S1A of the Supporting Information); these transformed cells were able to grow in low-serum media (Figure S1B of the Supporting Information), and they formed foci in culture dishes (Figure S1C of the Supporting Information). Overexpression of rat p67/MetAP2 in these transformed fibroblasts showed subsequent inhibition of growth rates, serum independence, and formation of foci (Figure S1A–C of the Supporting Information). Collectively, these data suggest that rat p67/MetAP2 has the ability to suppress K-rasV12-mediated transformed phenotypes of NIH3T3 fibroblasts in culture and in athymic nude mice.

Rat p67/MetAP2 Binds Directly to ERK1/2 MAP Kinases in Vivo and in Vitro. However, Its Binding to MEK1/2 May Be Indirect. To confirm whether the suppression of the tumor phenotype in K-RasV12-transformed mouse NIH3T3 fibroblasts is due to direct binding, we performed GST pull-down assays (Figure 5A–J). Purified GST protein or its fusion of the N-terminal segment of residues 1–80 of rat p67/MetAP2 showed no binding to either ERK1 (Figure 5A,I, lanes 1 and 2) or ERK2 (Figure 5C,J, lanes 1 and 2); GST fusions of residues 71–150 of rat p67/MetAP2 showed stronger binding to ERK1 as compared to other segments, residues 141–220, 211–290, 281–336, and 340–430 (compare lanes 3 with lanes

4–7 in Figure 5A,I). In parallel experiments, GST fusions of N-terminal residues 71–150 and C-terminal residues 281–336 and 340–430 of rat p67/MetAP2 showed weaker binding with ERK2 than residues 141–220 and 211–290 (compare lanes 3, 6, and 7 with lanes 4 and 5 in Figure 5C,J). In reciprocal experiments, full-length rat p67/MetAP2 binds to neither glutathione agarose beads (Figure 5F, lane 1) nor purified GST (Figure 5F, lane 2). However, it binds strongly to full-length ERK2 and its segments spanning amino acid residues 1–300 and 1–98 (Figure 5F, lanes 3–5) and weakly to residues 1–150 of ERK2 (lane 6), and no binding was detected with N-terminal residues 1–75 of ERK2 (Figure 5F, lane 7). The ERK2 segments spanning amino acid residues 76–358 and 151–358 also showed strong binding with p67/MetAP2 (data not shown). We performed similar GST pull-down experiments with ERK1 fragments and obtained similar results as shown for ERK2 in Figure 5F–H (data not shown). Altogether, our data suggest that rat p67/MetAP2 directly binds to both ERK1 and ERK2. Our co-immunoprecipitation data (Figure S2A–H of the Supporting Information) and semi-in vitro binding data (Figure S3A–E of the Supporting Information) further confirmed the binding regions within p67/MetAP2 and ERK1/2 as observed from in vitro binding experiments. Regardless of whether this binding has any role in the autoproteolysis of rat p67/MetAP2, we examined the effects of overexpression of ERK1 or ERK2 in p67/MetAP2's autocleavage (Figure S4 of the Supporting Information). The Myc-tagged rat p67/MetAP2 cleaves into fragments when ectopically expressed in C2C12 myoblasts or in NIH3T3 fibroblasts (Figure S4 of the Supporting Information,

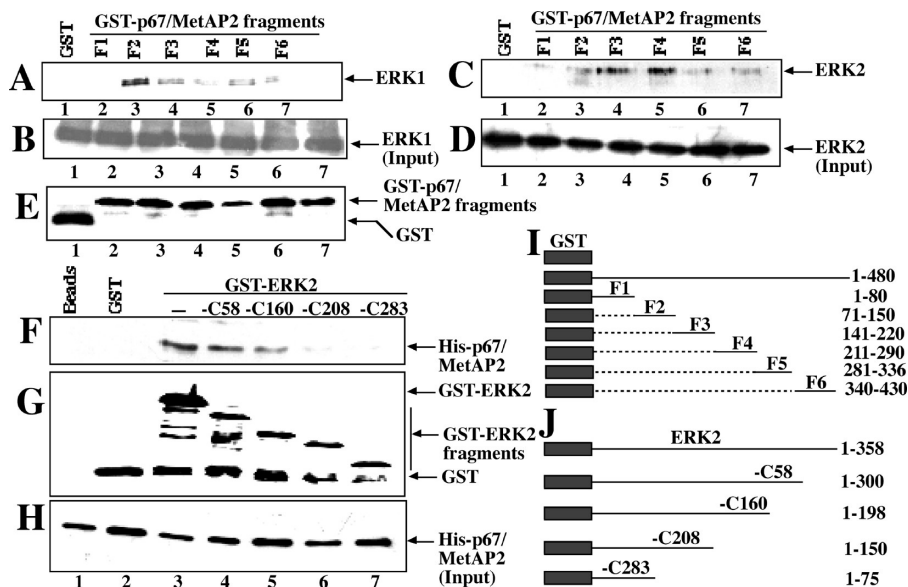


FIGURE 5: N-terminal residues 1–150 and residues 141–290 of rat p67/MetAP2 bind in vitro to ERK1 and ERK2, respectively, whereas N-terminal residues 1–150 of ERK2 show no binding to rat p67/MetAP2 in vitro. GST pull-down assays were performed using different purified glutathione *S*-transferase (GST)-tagged fragments of rat p67/MetAP2 (0.5 μg each) and 100 ng each of purified ERK1 and ERK2. Western blot analyses were conducted for the detection of ERK1 (A), ERK2 (C), input ERK1 (B), input ERK2 (D), and GST fusions of rat p67/MetAP2 fragments (E) using appropriate antibodies for these proteins. Similar GST pull-down assays were performed with purified GST-tagged ERK2 and its fragments (residues 1–300, 1–198, 1–150, and 1–75) (0.5 μg each) and 200 ng of purified His-tagged rat p67/MetAP2. Western blot analyses were performed for the detection of bound p67/MetAP2 (F), GST fusions of ERK2 and its fragments (G), and input His-tagged rat p67/MetAP2 (H) using monoclonal antibodies specific for the His tag (F and H) and the GST tag (G). Schematic representations of the different fragments (F1–F6) of rat p67/MetAP2 and ERK2 are shown in panels I and J, respectively.

lane 1 in both panels A and B), and this cleavage was inhibited when either ERK1 or ERK2 was co-expressed with rat p67/MetAP2 (Figure S4 of the Supporting Information, lanes 2 and 3 in panel A and lane 2 in panel B, respectively). Altogether, these results suggest that the p67/MetAP2's autoproteolysis was inhibited by ERK1/2 because of their direct interactions.

To examine the effect(s) of p67/MetAP2's direct binding to the activity of ERK1 and ERK2, we phosphorylated myelin basic protein (MBP) with either purified ERK1 (Figure 6A) or ERK2 (Figure 6D) in in vitro kinase assays (lane 1 in both panels A and D of Figure 6). This phosphorylation was inhibited by more than 90% when purified His-tagged full-length rat p67/MetAP2 was added to the kinase reaction mixture prior to the addition of ERK1 (Figure 6A,C, lane 2), but only 20 and 15% inhibition was observed when either p52 or p26 of rat p67/MetAP2, respectively, was added to the ERK1 kinase reaction mixture (Figure 6A,C, lanes 3 and 4). Amounts of input ERK1 were basically the same in these kinase reactions (Figure 6B, lanes 1–4). On the other hand, the level of phosphorylation of MBP by purified ERK2 was reduced to 5% when His-tagged purified rat p67/MetAP2 was added to the reaction mixture prior to the addition of ERK2 kinase (in Figure 6D,F, compare lanes 1 and 2). The addition of the purified His-tagged p52 or p26 fragment of rat p67/MetAP2 to the ERK2 kinase assays reduced the level of phosphorylation of MBP by 30 or 25%, respectively (in Figure 6D,F, compare lanes 3 and 4 with lane 1). The amounts of input ERK2 were basically the same in these kinase reactions (Figure 6E, lanes 1–4). The amounts of purified His-tagged full-length rat p67/MetAP2 and its fragments p52 and p26 added to the kinase reaction mixtures are shown in Figure 6G, whereas the amounts of MBP used in these experiments are shown in Figure 7H. It is, however, noticeable that the molar ratios of p52 and p26 added to the reaction mixtures were slightly more than the amount of

full-length rat p67/MetAP2 (in Figure 6G, compare lanes 3 and 4 with lane 2). Nonetheless, these data suggest that both the N-terminal p26 fragment and the downstream C-terminal p52 segment of rat p67/MetAP2 are essential for the inhibition of activity of ERK1 and ERK2 in vitro. In these studies, we have used MBP as an artificial substrate, which has been routinely used for testing in vitro kinase assays for ERK1/2 (30).

In our earlier experiments (Figures 1 and 3), we observed that p67/MetAP2 inhibits both the activation and activity of ERK1/2 MAP kinases. In addition, it also inhibits the phosphorylation of MEK (Figure 4A), the upstream activator of ERK1/2 MAP kinases (9, 17). We therefore explored whether p67/MetAP2 binds to MEK1 in mouse C2C12 myoblasts and NIH3T3 fibroblasts via co-immunoprecipitation assays (Figure S5A–R of the Supporting Information). After a series of co-immunoprecipitation assays and GST pull-down assays, we have concluded that binding between MEK1/2 and p67/MetAP2 may be through ERK1/2 MAP kinases, which bind to MEK1/2 very tightly.

Endogenous p67/MetAP2 Is Required To Suppress the Phosphorylation of ERK1/2 MAP Kinases in both C2C12 Myoblasts and NIH3T3 Fibroblasts. Earlier, we have demonstrated that ectopic expression of rat p67/MetAP2 in either mouse NIH3T3 fibroblasts or C2C12 myoblasts inhibits the activation and activity of ERK1/2, and this inhibition indeed was propagated into the downstream targets of ERK1/2 (Figure 4). We have also demonstrated that p67/MetAP2 binds to the endogenous ERK1/2 (4, 10, 11) (Figure 5). To examine whether the endogenous mouse p67/MetAP2 is involved in the maintenance of the activation and activity of ERK1/2 MAP kinases in C2C12 myoblasts and in NIH3T3 mouse fibroblasts, we knocked down the levels of p67/MetAP2 using siRNA (Figure 7A), keeping the GFP level unchanged (Figure 7B). This siRNA sequence corresponds to the lysine residue-rich domain I (4), and

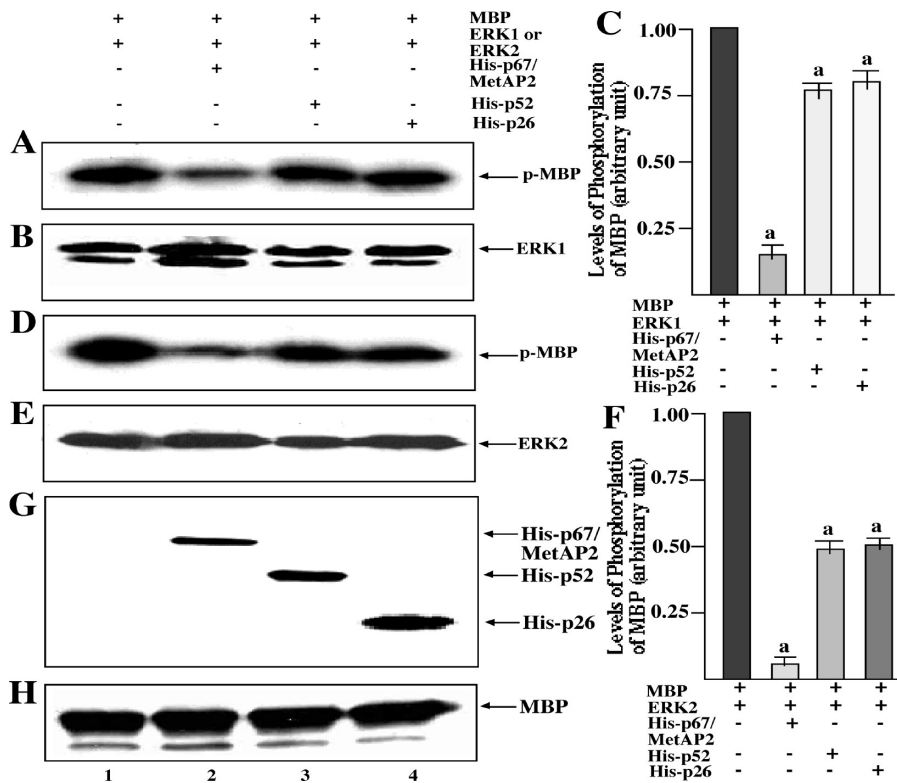


FIGURE 6: Both p52 and p26 fragments of rat p67/MetAP2 are required for the inhibition of activity of ERK1 and ERK2 in vitro. In an in vitro ERK1 kinase assay, the activated ERK1 (200 ng) was mixed with 0.5 μ g of myelin basic protein (MBP) in kinase buffer and incubated at 30 °C for 30 min after addition of 10 μ Ci of [γ -³²P]ATP alone (lane 1) or in the presence of 0.5 μ g each of His-tagged full-length rat p67/MetAP2 (lane 2) or its fragments, p52 (lane 3) and p26 (lane 4). The reactions were stopped by addition of SDS-PAGE loading dye and boiled for 5–10 min followed by analyses of a 15% SDS-PAGE gel and autoradiography (A). Proteins from the gel were transferred to a nitrocellulose membrane and analyzed via Western blots using polyclonal antibodies specific for ERK1 (B) and a monoclonal antibody specific for the His epitope (C). A similar analysis was performed and the sample stained with Coomassie blue for the detection of MBP (D).

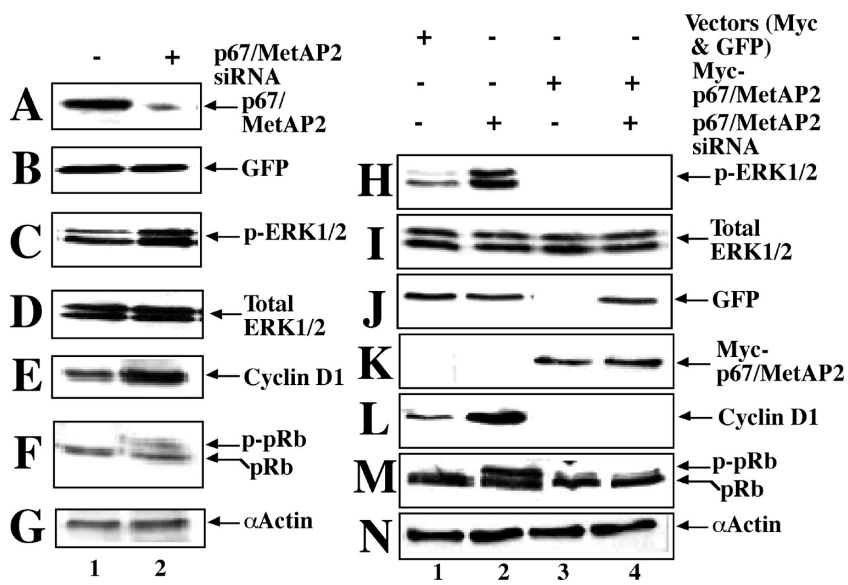


FIGURE 7: p67/MetAP2 is required for the suppression of the activation and activity of ERK1/2 MAP kinases during normal growth conditions. C2C12 myoblasts (50–60% confluent) were transiently transfected with a plasmid expressing p67/MetAP2 siRNA (4). Twenty-eight hours after transfection, cell lysates were made and analyzed on Western blots for the levels of p67/MetAP2 (A), green fluorescence protein (GFP) (B), phosphorylated forms of ERK1/2 (C), total ERK1/2 (D), cyclin D1 (E), pRb (F), and α -actin as a loading control (G) using appropriate antibodies as shown in the respective panels. C2C12 myoblasts were also transiently transfected with the Myc and GFP vectors (2.5 μ g each) (H, lane 1) or expressed p67/MetAP2 siRNA (H, lane 2). Into the C2C12 cells was introduced a plasmid (5 μ g) expressing Myc-tagged p67/MetAP2 alone or in combination with another plasmid (5 μ g) expressing p67/MetAP2 siRNA through transient transfection. Cell lysates from these transfected cells were analyzed on Western blots for the levels of the phosphorylated forms of ERK1/2 (H), total ERK1/2 (I), GFP (J), Myc-p67/MetAP2 (K), cyclin D1 (L), pRb and pp-Rb (M), and α -actin as a loading control (N) using the appropriate antibodies as shown in the respective panels.

this sequence is 100% conserved within mammals, including mouse, rat, and human (2). We noticed that lowering the mouse

p67/MetAP2 level caused the increased level of phosphorylation of ERK1 and ERK2 (Figure 7C), keeping its total level

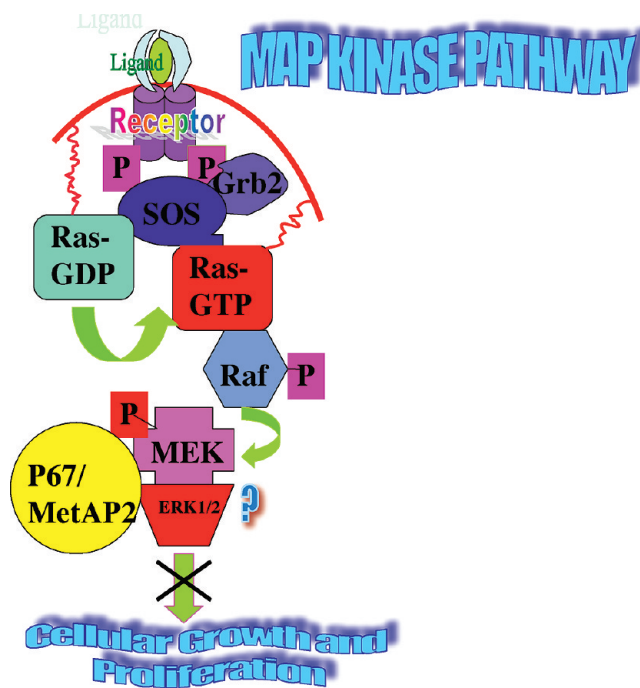


FIGURE 8: Tentative working model. A schematic representation of the ERK1/2 MAP kinase pathway that shows the specific site for p67/MetAP2's action to inhibit cell growth by inhibiting the activation and activity of ERK1/2 MAP kinases.

unchanged (Figure 7D), and subsequently, the level of cyclin D1 increased (Figure 7E) and the level of phosphorylation of pRb also increased (Figure 7F). In the p67/MetAP2 siRNA-expressing cells when rat p67/MetAP2 was co-expressed along with its siRNA, siRNA's effect on increasing the levels of p-ERK1/2 was significantly weakened (Figure 7H,I), and subsequent downstream targets like the levels of cyclin D1 and pp-Rb were also affected (Figure 7L,M). The exogenous rat p67/MetAP2 level was near 40–50% of the endogenous level of its mouse homologue (data not shown). Among several downstream targets for ERK1 and ERK2, cyclin D1 and pRb are the downstream targets that regulate the cell cycle (22, 29). Therefore, the increased levels of cyclin D1 and increased level of phosphorylation of pRb are due to the increased level of phosphorylation of ERK1/2. We have also performed similar knock-down studies using the above p67/MetAP2 siRNA in rat tumor hepatoma (KRC-7) cells, mouse NIH3T3 fibroblasts, and HeLa cells with similar results (data not shown). Altogether, these results suggest that endogenous p67/MetAP2 is also involved in the maintenance of the phosphorylation levels of ERK1/2 MAP kinases in mammalian cells from mouse, rat, and human.

DISCUSSION

The ERK1/2 MAP kinase-mediated signaling pathway regulates cell growth and proliferation and thus plays a major role in cell cycle regulation. The proto-oncogene product, Ras, is the master regulator of this signaling pathway (22). Among three highly conserved Ras genes, H-, K-, and N-Ras, the high potential of K- and N-Ras to activate the ERK pathway correlates with the higher frequency of mutation in K-and N-Ras than in H-Ras (23, 24). A K-Ras mutation is commonly found in more than 60% of human cancers (9), and constitutive expression of K-RasV12, a mutant form of K-Ras, in NIH3T3 mouse fibroblasts leads to tumor formation in culture cells

[Figure 1 (17)] and in xenograft mice (Figure 2) by activating the Ras-Raf-MEK-ERK1/2 signaling pathway [Figure 1 (14)]. Overexpression of rat p67/MetAP2 in K-RasV12-mediated NIH3T3 transformed cells suppresses the tumorigenic phenotype both in culture (Figure 1) and in athymic nude mice (Figure 2). This suppression is due to the inhibition of the activation and activity of ERK1/2 MAP kinases through protein–protein interactions (Figures 1 and 3 and Figures S3–S6 of the Supporting Information). Overexpression of rat p67/MetAP2 not only inhibits the induced activation of MEK, an upstream activator of ERK1/2 MAP kinases (Figure 3), but also inhibits the activation of RSK and expression of cyclin D1 (Figure 4), which are the downstream targets of ERK1/2 MAP kinases, and shows tumor suppression ability both in cell culture and in athymic nude mice (Figures 1 and 2). The inhibition of activity of ERK1/2 by p67/MetAP2 (Figure 6) is due to its direct binding with these MAP kinases (Figures S2, S3, and S5 of the Supporting Information). The effects on phosphorylation of MEK, the upstream activator of ERK1/2 MAP kinases, due to overexpression of rat p67/MetAP2 (Figure 4A), may not be direct. In our future experiments, we will explore in detail the interactions between p67/MetAP2 and MEK1/2 by using different conditions and cell types and examine the effects on addition of p67/MetAP2 in MEK1-mediated phosphorylation of ERK1/2 MAP kinases in *in vitro* phosphorylation assays. Dual inactivation of MEK and ERK1/2 by rat p67/MetAP2 is due to the formation of a multiprotein complex consisting of MEK, ERK1/2, and rat p67/MetAP2 (Figure S5 of the Supporting Information), and this leads to cell growth inhibition via inactivation of the Ras-Raf-MEK-ERK MAP kinase signaling pathway (Figure 8).

P67/MetAP2's inhibition of the activation and activity of ERK1/2 MAP kinases may propagate to multiple directions in cell signaling pathways. For example, inhibition of RSK phosphorylation could have an effect on tuberin's function. Tuberin represents a major signal integrator receiving multiple inputs from the Ras and PI-3K pathways. RSK1 interacts with and phosphorylates tuberin at a regulatory site, Ser-1798 located at its evolutionarily conserved C-terminus (31). This phosphorylation of tuberin inhibits the tumor suppressor function of the tuberin–hamartin complex (31). Inhibition of RSK phosphorylation by rat p67/MetAP2 could have activated the tumor suppression activity of tuberin. Another downstream effector of ERK1/2 MAP kinases is cyclin D1 (29). The increased level of expression of cyclin D1 in K-RasV12-transformed NIH3T3 cells correlates with its ability to induce G1 progression (29). Amplification and overexpression of cyclin D1 have been reported in various tumors, including non-small-cell lung carcinomas and hepatocellular carcinomas (29). In addition, recent evidence suggests that overexpression of cyclin D1 is an early causative event in hepatocarcinogenesis (29). Rat p67/MetAP2's ability to inhibit the phosphorylation of RSK and cyclin D1's expression through the inactivation of ERK1/2 MAP kinases (Figure 4) in K-RasV12-transformed NIH3T3 cells support the notion that rat p67/MetAP2 may have tumor suppression activity either directly or indirectly. This idea was further supported by the observations that overexpression of rat p67/MetAP2 in K-RasV12-mediated transformed NIH3T3 fibroblasts led to the suppression of proliferation, the inhibition of the ability to grow in low serum, and the formation of foci under *ex vivo* conditions (Figure S1 of the Supporting Information). In addition, it can suppress tumor growth in athymic mice, which formed highly aggressive, invasive, and solid tumors when

K-RasV12-mediated transformed cells were injected. However, less aggressive, less invasive, and spongy types of tumors were seen in athymic mice treated with K-RasV12-transformed NIH3T3 fibroblasts overexpressing p67/MetAP2 (Figure 2).

There are several negative regulators of the Ras pathway in cells. Among them, sprouty, a Ras suppressor in *Drosophila*, and its mammalian homologue, Spred, function as negative feedback regulators of the ERK1/2 MAP kinase pathways (32). The Ras effector protein, RIN1, also inhibits Ras-induced activation of Raf by competitively binding with active Ras (33). The RIN1 gene is silent in breast tumor cell lines, and its expression inhibits the initiation and progression of tumorigenesis for breast tumor cell lines in a mouse model, consistent with its tumor suppressor activity (34). Erbin is also a negative regulator of ERK1/2 MAP kinase pathways. It binds to the active Ras and inhibits its association with Raf (35). The negative regulators provide a checkpoint control to ensure appropriate balance between normal cell growth and cancerous cell growth. The negative regulators mentioned above can also balance the overamplification of the proliferative signal caused by the Ras mutation that is present in 40–50% of human cancers (9, 23, 24). These negative regulators are therefore considered as tumor suppressors. Our study suggests that rat p67/MetAP2 also functions as a negative regulator of ERK1/2 MAP kinase pathways, and therefore, it is a novel tumor suppressor. Tumor suppression activity of several proteins has been implicated as an emerging alternative for the treatment of cancer (36–39). Rat p67/MetAP2's unique ability to suppress K-RasV12-mediated tumorigenesis in athymic mice raises several questions regarding its applicability in the treatment of cancer through gene therapy.

ACKNOWLEDGMENT

We thank Drs. Andrew Catling and Scott Eblen (University of Texas at San Antonio) for their generous gift of Flag-tagged ERK1 and ERK2 plasmids, Dr. Natalie Ann (University of Colorado) for her generous gift of the HA-tagged MEKA plasmid, and Dr. Alan Wolfman (Cleveland Clinic Foundation) for his generous gift of the pZip-K-RasV12 plasmid. We also thank Mrs. Rekha Datta for her excellent technical assistance.

SUPPORTING INFORMATION AVAILABLE

Inhibition of growth rates and formation of foci of K-RasV12-transformed NIH3T3 fibroblasts due to overexpression of rat p67/MetAP2 (Figure S1), in vivo binding of p67/MetAP2 with ERK1/2 MAP kinases (Figure S2), semi-in vitro binding of ERK1/2 with full-length rat p67/MetAP2 and its fragments, p26 and p52 (Figure S3), inhibition of autoproteolysis of rat p67/MetAP2 due to overexpression of ERK1/2 (Figure S4), and in vivo binding between p67/MetAP2 and ERK1/2 MAP kinases and MEK1/2 via co-immunoprecipitation assays (Figure S5). This material is available free of charge via the Internet at <http://pubs.acs.org>.

REFERENCES

- Folkman, J. (2007) Angiogenesis: An organizing principle for drug discovery? *Nat. Rev. Drug Discovery* 6, 273–286.
- Datta, B. (2009) Roles of p67/MetAP2 as a tumor suppressor. *Biochim. Biophys. Acta* 1796, 281–292.
- Ingber, D., Fujita, T., Kishimoto, S., Sudo, K., Kanamaru, T., Brem, H., and Folkman, J. (1990) Synthetic analogues of fumagillin that inhibits angiogenesis and suppress tumour growth. *Nature* 348, 555–557.
- Datta, B., Majumdar, A., Datta, R., and Balusu, R. (2004) Treatment of cells with the angiogenic inhibitor fumagillin results in increased stability of eukaryotic initiation factor 2 associated glycoprotein, p67, and reduced phosphorylation of extracellular signal-regulated kinases. *Biochemistry* 43, 14821–14831.
- Wang, J., Lou, P., and Henkin, J. (2000) Selective inhibition of endothelial cell proliferation is not due to differential expression of methionine aminopeptidases. *J. Cell. Biochem.* 77, 465–473.
- Griffith, E. C., Su, Z., Niwayama, S., Ramsay, C. A., Chang, Y. W., Wu, Z., and Liu, Z. O. (1998) Molecular recognition of angiogenesis inhibitors fumagillin and ovalicin by methionine aminopeptidase 2. *Proc. Natl. Acad. Sci. U.S.A.* 95, 15183–15188.
- Liu, S., Widom, J., Kemp, C. W., Crews, C. M., and Clardy, J. (1998) Structure of human methionine aminopeptidase-2 complexed with fumagillin. *Science* 282, 1324–1327.
- Datta, B., Ghosh, A., Majumdar, A., and Datta, R. (2007) Autoproteolysis of rat p67 generates several peptide fragments: The N-terminal fragment, p26, is required for the protection of eIF2α from phosphorylation. *Biochemistry* 46, 3465–3475.
- Raman, R., Chen, W., and Cobb, M. H. (2007) Differential regulation and properties of MAPKs. *Oncogene* 26, 3100–3112.
- Datta, B., Datta, R., Ghosh, A., and Majumdar, A. (2004) Eukaryotic initiation factor 2-associated glycoprotein, p67, shows differential effects on the activity of certain kinases during serum-starved conditions. *Arch. Biochem. Biophys.* 427, 68–78.
- Datta, B., Datta, R., Ghosh, A., and Majumdar, A. (2005) The stability of eukaryotic initiation factor 2-associated glycoprotein, p67, increases during skeletal muscle differentiation and that inhibits the phosphorylation of extracellular signal-regulated kinases 1 and 2. *Exp. Cell Res.* 303, 174–182.
- Ghosh, A., Datta, R., Majumdar, A., Bhattacharya, M., and Datta, B. (2006) The N-terminal lysine residue-rich domain II and the 340–430 amino acid segment of eukaryotic initiation factor 2-associated glycoprotein p67 are the binding sites for the γ-subunit of eIF2. *Exp. Cell Res.* 312, 3184–3202.
- Ray, M. K., Chakraborty, A., Datta, B., Chattopadhyay, A., Saha, D., Bose, A., Kinzy, T. G., Wu, S., Hileman, R. E., Merrick, W. C., and Gupta, N. K. (1993) Characterization of eukaryotic initiation factor 2-associated 67-kDa polypeptide. *Biochemistry* 32, 5151–5159.
- McKay, M. M., and Morrison, D. K. (2007) Integrating signals from RTKs to ERK/MAPK. *Oncogene* 26, 3113–3121.
- Giehl, K. (2005) Oncogenic Ras in tumour progression and metastasis. *Biol. Chem.* 386, 193–205.
- Gollob, J. A., Wilhelm, S., Carter, C., and Kelley, S. L. (2006) Role of Raf kinase in cancer: Therapeutic potential of targeting the Raf/MEK/ERK signal transduction pathway. *Semin. Oncol.* 33, 392–406.
- Mansour, S. J., Matten, W. T., Hermann, A. S., Candia, J. M., Rong, S., Fukasawa, K., Vande Woude, G. F., and Ahn, N. G. (1994) Transformation of mammalian cells by constitutively active MAP kinase kinase. *Science* 265, 966–970.
- Roberts, P. J., and Der, C. J. (2007) Targeting the Raf-MEK-ERK mitogen-activated protein kinase cascade for the treatment of cancer. *Oncogene* 26, 3291–3310.
- Datta, B., Datta, R., Ghosh, A., and Majumdar, A. (2006) The binding between p67 and eukaryotic initiation factor 2 plays important roles in the protection of eIF2α from phosphorylation by kinases. *Arch. Biochem. Biophys.* 452, 138–148.
- Datta, R., Choudhury, P., Bhattacharya, M., Leon, F. S., Zhou, Y., and Datta, B. (2001) Protection of translation initiation factor eIF2 phosphorylation correlates with eIF2-associated glycoprotein p67 levels and requires the lysine-rich domain I of p67. *Biochimie* 83, 919–931.
- Petush, S. F., Garcia, U., Haber, M. M., Katsinis, C., and Tozeren, A. (2006) Large-scale computations on histology images reveal grade-differentiating parameters for breast cancer. *BMC Med. Imaging* 6, 14–18.
- Meloche, S., and Pouyssegur, J. (2007) The ERK1/2 mitogen-activated protein kinase pathway as a master regulator of the G1- to S-phase transition. *Oncogene* 26, 227–3239.
- Cox, A. D., and Der, C. J. (2002) Ras family signaling. *Cancer Biol. Ther.* 1, 599–606.
- Wennerberg, K., Rossman, K. L., and Der, C. J. (2005) The Ras superfamily at a glance. *J. Cell Sci.* 118, 843–846.
- Kolch, W. (2005) Coordinating ERK/MAPK signaling through scaffolds and inhibitors. *Nat. Rev. Mol. Cell Biol.* 6, 827–837.
- Anjum, R., and Blenis, J. (2008) The RSK family of kinases: Emerging roles in cellular signalling. *Nat. Rev. Mol. Cell Biol.* 9, 747–758.
- Frödin, M., and Gammeltoft, S. (1999) Role and regulation of 90 kDa ribosomal S6 kinase (RSK) in signal transduction. *Mol. Cell. Endocrinol.* 151, 65–77.

28. Sassone-Corsi, P., Mizzen, C. A., Cheung, P., Crosio, C., Monaco, L., Jacquot, S., Hanauer, A., and Allis, C. D. (1999) Requirement of Rsk-2 for epidermal growth factor-activated phosphorylation of histone H3. *Science* 285, 886–891.
29. Gautschi, O., Ratschiller, D., Gugger, M., Betticher, D. C., and Heighway, J. (2007) Cyclin D1 in non-small cell lung cancer: A key driver of malignant transformation. *Lung Cancer* 55, 1–14.
30. Mandell, J. W., and Gocan, N. C. (2001) A green fluorescent protein kinase substrate allowing detection and localization of extracellular ERK/MAP kinase activity. *Anal. Biochem.* 293, 264–268.
31. Rosner, M., Hannerer, M., Siegel, N., Valli, A., and Hengstschläger, M. (2008) The tuberous sclerosis gene products hamartin and tuberin are multifunctional proteins with a wide spectrum of interacting partners. *Mutat. Res.* 658, 234–246.
32. Shaw, A. T., Meissner, A., Dowdle, J. A., Crowley, D., Magendantz, M., Ouyang, C., Parisi, T., Rajagopal, J., Blank, L. J., Bronson, R. T., Stone, J. R., Tuveson, D. A., Jaenisch, R., and Jacks, T. (2007) Sprouty-2 regulates oncogenic K-ras in lung development and tumorigenesis. *Genes Dev.* 21, 694–707.
33. Wang, Y., Waldron, R. T., Dhaka, A., Patel, A., Riley, M. M., Rozengurt, E., and Colicelli, J. (2002) The RAS Effector RIN1 Directly Competes with RAF and Is Regulated by 14-3-3 Proteins. *Mol. Cell. Biol.* 22, 916–926.
34. Milstein, M., Mooser, C. K., Hu, H., Fejzo, M., Slamon, D., Goodlick, L., Dry, S., and Colicelli, J. (2007) RIN1 is a breast tumor suppressor gene. *Cancer Res.* 67, 11510–11516.
35. Huang, Y. Z., Zang, M., Xiong, W. C., Luo, Z., and Mei, L. (2003) Erbin suppresses the MAP kinase pathway. *J. Biol. Chem.* 278, 1108–1114.
36. Chada, S., Menander, K. B., Bocangel, D., Roth, J. A., and Ramesh, R. (2008) Cancer targeting using tumor suppressor genes. *Front. Biosci.* 13, 1959–1967.
37. Khalighinejad, N., Hariri, H., Behnamfar, O., Yousefi, A., and Momeni, A. (2008) Adenoviral gene therapy in gastric cancer: A review. *World J. Gastroenterol.* 14, 180–184.
38. Torchilin, V. P. (2006) Recent approaches to intracellular delivery of drugs and DNA and organelle targeting. *Annu. Rev. Biomed. Eng.* 8, 343–375.
39. Thompson, N., and Lyons, J. (2005) Recent progress in targeting the Raf/MEK/ERK pathway with inhibitors in cancer drug discovery. *Curr. Opin. Pharmacol.* 5, 350–356.